Published in final edited form as:
J Cogn Neurosci. 2011 June ; 23(6): 1507–1521. doi:10.1162/jocn.2010.21534.

Neural Activity in Frontal Cortical Cell Layers: Evidence for Columnar Sensorimotor Processing

Ioan Opris[*], **Robert E. Hampson**, **Terrence R. Stanford**[**], **Greg A. Gerhardt**[***], and **Sam A. Deadwyler**
Wake Forest University Medical School, Winston-Salem, NC

Abstract

The mammalian frontal cortex (FCx) is at the top of the brain's sensorimotor hierarchy and includes cells in the supragranular Layer 2/3, which integrate convergent sensory information for transmission to infragranular Layer 5 cells to formulate motor system outputs that control behavioral responses. Functional interaction between these two layers of FCx was examined using custom-designed ceramic-based microelectrode arrays (MEAs) that allowed simultaneous recording of firing patterns of FCx neurons in Layer 2/3 and Layer 5 in nonhuman primates performing a simple *go/no-go* discrimination task. This unique recording arrangement showed differential encoding of task-related sensory events by cells in each layer with Layer 2/3 cells exhibiting larger firing peaks during presentation of *go target* and *no-go target* task images, whereas Layer 5 cells showed more activity during reward contingent motor responses in the task. Firing specificity to task-related events was further demonstrated by synchronized firing between pairs of cells in different layers that occupied the same vertically oriented "column" on the MEA. Pairs of cells in different layers recorded at adjacent "noncolumnar" orientations on the MEA did not show synchronized firing during the same task-related events. The results provide required evidence in support of previously suggested task-related sensorimotor processing in the FCx via functionally segregated minicolumns.

INTRODUCTION

The sensorimotor neural processing system of the primate brain is crucial for the guidance of planned and learned behaviors (Andersen & Buneo, 2003; Fadiga & Craighero, 2003; Caminiti, Ferraina, & Mayer, 1998; Crammond & Kalaska, 1994; di Pellegrino & Wise, 1993; Mushiake, Inase, & Tanji, 1991). The frontal cortex (FCx) occupies the summit of sensorimotor processing hierarchies in the primate brain and plays a key role in the integration of sensory signals and their transformation into motor plans for action (Opris & Bruce, 2005; Schwartz, Moran, & Reina, 2004; Lebedev, Messinger, Kralik, & Wise, 2002; Fuster, 2001; Miller & Cohen, 2001; Boussaoud & Wise, 1993; Passingham, 1993; Rizzolatti et al., 1987; Kubota & Komatsu, 1985; Wise, 1985). Such transformation of incoming sensory information in the FCx and pFC is via normally firing "regular-spiking" (RS) layer-specific pyramidal cells and "fast-spiking" (FS) interneurons located within each cortical layer (Rao, Williams, & Goldman-Rakic, 1999). It has been shown in rodents and nonhuman primates (NHPs) that both types of cells are embedded in "laminar" microcircuits

Reprint requests should be sent to Dr. Sam A. Deadwyler, Department of Physiology and Pharmacology, Wake Forest University School of Medicine, Medical Center Boulevard, Winston Salem, NC 27157, or via sdeadwyl@wfubmc.edu.
[*]Current Address: Department of Neurobiology, Duke University Medical Center, Durham, NC.
[**]Current Address: Department of Anatomy and Neurobiology, Wake Forest University Medical School, Winston-Salem, NC.
[***]Current Address: Department of Anatomy and Neurobiology, University of Kentucky, Lexington, KY.

that consist of layered “minicolumns,” interconnected via projections of pyramidal cells to larger networks in other cortical and subcortical brain regions (Weiler, Wood, Yu, Solla, & Shepherd, 2008; Dombrowski, Hilgetag, & Barbas, 2001; Mountcastle, 1997; Kritzer & Goldman-Rakic, 1995; Barbas & Pandya, 1987, 1989). Such FCx minicolumns consist of cells in supragranular Layer 2/3, which receive convergent synaptic inputs from sensory and motor systems, and cells in the infragranular Layer 5, which are hypothesized to supply local circuit outputs to subcortical structures that mediate planned behavioral responses (Takeda & Funahashi, 2006; Yoshimura, Dantzker, & Callaway, 2005; Melchitzky, Sesack, Pucak, & Lewis, 1998; Kritzer & Goldman-Rakic, 1995).

A question posed early on (Mountcastle, 1997; Lorente de No, 1949) and that has remained somewhat unresolved (Weiler et al., 2008; Yoshimura et al., 2005; Douglas & Martin, 2004) is, “What are the transforming operations imposed in a local region of neocortex, a cortical column, upon its input, to produce its targeted outputs?” Previous anatomic and electrophysiological investigations (Funahashi & Inoue, 2000; González-Burgos, Barrionuevo, & Lewis, 2000; Jung, Qin, McNaughton, & Barnes, 1998; Kritzer & Goldman-Rakic, 1995) have examined both the structural and the functional bases of this operation (de Kock, Bruno, Spors, & Sakmann, 2007; Sakurai & Takahashi, 2006; Opris, Barborica, & Ferrera, 2005; Constantinidis, Williams, & Goldman-Rakic, 2002; Constantinidis, Franowicz, & Goldman-Rakic, 2001; Kritzer & Goldman-Rakic, 1995), but only a few studies have examined simultaneous firing patterns of cells in different cortical layers (Derdikman et al., 2006; Zhang & Alloway, 2006; Krupa et al., 2002; Jung et al., 1998).

The goal of the research reported here was to assess the columnar and laminar features of sensorimotor processing within Areas 46, 8, and 6 of FCx using a custom-designed ceramic-based microelectrode array (MEA; Burmeister et al., 2008; Hampson, Coates, Gerhardt, & Deadwyler, 2004; Moxon, Leiser, Gerhardt, Barbee, & Chapin, 2004) capable of recording simultaneous firing patterns of cells in Layer 2/3 and Layer 5 in NHPs performing a *go/no-go* visual discrimination task (Opris, Hampson, & Deadwyler, 2009). It is likely that RS and FS cells within each column show segregated activation and lack of integration across cortical layers if the columnar arrangement is to be maintained during different types of sensorimotor processing (Weiler et al., 2008; Goldman-Rakic, 1995). The custom-designed conformal MEA used in this study provides four separate recording sites at two different vertical depths corresponding to the distance between these two FCx layers (Hampson, Coates, et al., 2004). The results indicate that FCx neurons in Layer 2/3 and Layer 5 differentially encode task-related sensory stimuli and that such firing are segregated with respect to narrow bands of columnar-like synchronized activity across both layers evidenced by the spatially distinct recording sites on the conformal MEAs.

METHODS

All animal procedures were reviewed and approved by the Institutional Animal Care and Use Committee of Wake Forest University, in accordance with guidelines of the U.S. Department of Agriculture, the American Association of Laboratory Animal Care, the National Institutes of Health, and the U.S. Army Medical Research and Materiel Command Animal Care and Use Review Office.

Surgery

Each of the three NHPs (*Macacamulatta*) was anesthetized with ketamine (10 mg/kg) then intubated and maintained with isoflurane (1–2% in oxygen 6 l/min) during surgical placement of recording cylinders over targeted areas of FCx (Figure 1). The recording cylinders (Crist Instruments) were mounted on the skull over 11 mm diameter craniotomies for MEA access to frontal cortical recording loci (Opris et al., 2009; Hampson, Pons,

Stanford, & Deadwyler, 2004). Cylinder placement was determined by MRI to overlie FCx at stereotaxic coordinates 25 mm anterior to interaural line and 12 mm lateral to the midline (Paxinos, Huang, & Toga, 2000). This location allowed access to the caudal region of principal sulcus, the dorsal limb of arcuate sulcus in area 8, and the dorsal premotor area 6 (Figure 1A). Two titanium posts were secured to the skull for head restraint with titanium screws embedded in bone cement. After surgery, animals were given 0.025 mg/kg buprenorphine for analgesia and penicillin injections to prevent infection. All cylinders were cleaned with Betadine after surgery and routinely during daily recording sessions.

Recording Procedures

Data acquisition software for 64-channel simultaneous recordings used the MAP Spike Sorter by Plexon, Inc. (Dallas, TX). RS and FS neurons (Elston et al., 2006; Rao et al., 1999) were recorded in Layer 2/3 and Layer 5 and from the dorsal bank of the arcuate sulcus in the dorsolateral premotor area of FCx. Custom-made ceramic MEAs, designed collaboratively and manufactured at the Center for Microelectrode Technology, University of Kentucky, consisted of eight patterned platinum recording pads on a ceramic substrate (Figure 1D and E) specifically configured for recording single neuron activity (Hampson, Coates, et al., 2004; Moxon et al., 2004). The model W3 version of the MEAs (Figure 1D and E) was specially designed with 20 × 150-μm recording pads 2a–d located to record activity from supragranular (Layer 2/3) cells, whereas pads 5a–d simultaneously recorded neuron activity from infragranular Layer 5 neurons (Figure 1B). The intrapad distance between the edges of pads 2a–d and 5a–d was 1350 μm, with a 40-μm separation between adjacent pads (i.e., 2a–c, 2b–d, etc.). Extracellular neuron action potentials (spikes) were identified and isolated on-line by separation of extracellular action potential waveform duration and amplitude and confirmed via off-line analysis using principal components analysis and autocorrelation to confirm that (a) single neurons were isolated, (b) all spikes of a given neuron were identified within 95% confidence, and (c) neurons detected simultaneously on adjacent sites were counted only once. Neural spike trains were analyzed with respect to firing rate during specific events within go/no-go trials (Hampson, Pons, et al., 2004).

The Go/No-go Task

The three NHPs were trained to sit in primate chairs in front of a display screen and move a cursor with their right arm to perform a visually guided go/no-go task (Opris et al., 2009). The position of the right arm was tracked via an illuminated UV-fluorescent reflector affixed to the back of the hand, digitized, and displayed as a large yellow cursor on the projection screen. The go/no-go task involved placing the cursor into a *go target* image when it appeared on the screen for *go* trials or withholding the cursor from the *no-go target* image when it appeared on separate *no-go* trials (Figure 2A). Trials were initiated by the animals placing the cursor inside a 3-in. diameter circular yellow outline (“start ring”) in the center of the screen. Response to the start ring produced one of the two visually distinct target images (go or no-go) positioned at random locations on the screen. Movement of the cursor into the go target image for at least 500 msec, within 2.0 sec of presentation (*go response*), produced delivery of a squirt of juice via a sipper tube mounted next to the animal’s mouth on the chair (Hampson, Pons, et al., 2004). Presentation of the no-go target image required withholding the cursor from touching the image for a 5.0-sec interval (*no-go timeout*), after which a squirt of juice was automatically delivered via the sipper tube (Figure 2A). Incorrect responses (i.e., failure to respond to go target within 2.0 sec or touching the *no-go* image with the cursor during the 5.0-sec *no-go timeout* interval) were not rewarded and were followed by a 5.0-sec delay with the screen blanked and no trials. The go and no-go trials were presented randomly in equal numbers during the session, and all trials were separated

by a variable 3- and 10-sec intertrial interval). Animals were tested two to three times per week.

Data Analysis

Behavioral assessments of task performance were computed for each animal, yielding a mean for percent correct responses across all sessions for all animals of 93.8% (*SEM* = 0.5%), which indicated that prior training was sufficient to produce nearly automatic responding in the task with little or no cognitive demand (Figure 2A). Electrophysiological analyses used a MAP Spike Sorter (Plexon, Inc.) to discriminate and to analyze single-neuron waveforms from the MEAs in each animal with a multineuron acquisition processor and NeuroExplorer software (Nex Technologies, Littleton, MA). Mean firing rate for each neuron was analyzed in perievent histograms (PEHs) consisting of 100-msec time bins for ±3.0 sec surrounding each task-related event (e.g., image presentations and behavioral responses; Figure 2A). RS and FS neurons were segregated by frequency distribution of individual neuron baseline and peak firing rate into two distinct categories: one with baseline firing rate of 2 to 5 Hz with peaks to 10 Hz identified as RS cells, and the other category with baseline firing rates of 7 to 15 Hz and peaks >20 Hz identified as FS cells. In addition, neuron firing patterns were classified according to recording sites on the MEA as to layer identity and position (orientation) within the layer relative to neurons recorded in the other layer (Figure 1). Standard scores used the formula [z = (peak − baseline firing rate) / *SD* baseline firing rate] to identify significant firing peaks and/or troughs compared with baseline firing. For all analyses, baseline firing rate was computed as mean firing within a 1.0-sec epoch ending 1.0 sec before the presentation of the behavioral stimulus, that is, extending from −2.0 to −1.0 sec before the start ring, go target (presentation), or no-go target presentations. The go target response and reward were compared with the respective go or no-go target presentation baseline epoch to avoid including the neural response to the target. Only neurons with firing rates significantly elevated from baseline (Z scores, $p < .01$) were included in the analysis. Statistical analyses compared 600-msec time epochs for baselines, preevent, and postevent firing to test differences with respect to cells recorded in different layers (i.e., Layer 2/3 vs. Layer 5) and/or cells located at different sites on the MEA within the task. The synchrony between cells in different layers was tested using cross-correlation histograms (CCHs) that formulated the probability of synchronous spike occurrences using Layer 2/3 cell firing to test synchronous discharge of simultaneously recorded Layer 5 cells in 1.0-msec intervals over a ±2.0-sec time frame defined by significantly increased discharge to taskrelated events. CCHs were generated using a “shuffle 5 times” shift predictor built into Neuroexplorer, which computed the random cross-correlation due to chance by randomizing the actual spike sequence for a given pair of neurons. The randomization process was repeated four times, and random cross-correlation averaged over the five instances. This “shift-predictor” chance correlation was then subtracted from the raw correlation to produce CCHs. Population mean CCHs were then computed by averaging the CCHs across pairs of cells and plotting mean and *SEM* within 1-msec bins.

RESULTS

Neural activity was recorded with the abovementioned MEAs from cells in areas 46, 8, and 6 in the premotor region of FCx. Insertion methods and approaches were derived using MRI-confirmed stereotaxic coordinates to position MEAs perpendicular to the surface of the brain, which allowed simultaneous recording of cell activity in both Layer 2/3 and Layer 5 from multiple sites on the MEA (Figure 1). All animals were previously trained to perform the simple go/no-go task to near perfection (Figure 2A) to ensure differential behaviors during task-related events. Recordings were obtained from 253 frontal cortical neurons

during performance of the task in the three different NHPs (Animals 1, 2, and 3; n = 19, 135, and 99 cells, respectively) and pooled for analysis with respect to MEA recording pads and task events. Of these, 99 cells were recorded from Layer 2/3 (supragranular) and 154 cells from Layer 5 (infragranular). The behavioral recording context (Figure 2A) allowed simultaneous assessment of the role of frontal cortical cells located in these two layers during trained task-related overt motor responses. The recording probe design allowed assessment of functional differences in cells recorded from the two different laminar frontal cortical regions (layers) as a function of orthogonal (vertical) recording relations during the same behavioral events.

Frontal Cortical Cell Activity Recorded with Conformal Ceramic MEAs

Figure 2B shows examples of conformal array recording with the W3 MEAs in the dorsal premotor region during *go trials* of the go/no-go task. The waveforms recorded at the vertically separated (1350 μm) recording sites on the MEA indicate individual isolated neuron firing exhibiting task-related discharges within different cortical cell layers, presumably supragranular Layer 2/3 cells shown at locations 2a–d and infragranular Layer 5 cells shown at MEA site locations 5a–d. Corresponding PEHs in Figure 2B illustrate the firing patterns of the same neurons, identified in terms of MEA recording pad location (i.e., 2a, 2b, 5a, 5b, etc.), synchronized to *target* image presentations within the task. The MEA routinely recorded RS cells from both Layer 2/3 and Layer 5 simultaneously in the same session, and as indicated in Figure 2B, most cells showed a significant either increase or decrease (noted by asterisks) in activity related to go/no-go task events. Figure 2C shows a real-time strip chart of simultaneous recordings from sites 2a–c separated by 40 μm on the MEA probe. The record shows examples of extracellular action potentials (arrows) at both recording sites that were not detected at opposing MEA locations despite proximity, indicating a lack of electrical coupling between adjacent recording sites.

Frontal Cortical Cell Firing: Start Ring Presentation

Figure 3A shows two RS frontal cortical neurons (Elston et al., 2006) recorded in Layer 2/3 and 1350 μm deeper in Layer 5 at the respective pads (2a and 5a) on the MEA (shown at right). The raster displays and PEHs show firing over the entire (go target) trial before presentation of the start ring image to initiate the trial (red line at 0 sec) and subsequent firing throughout the remainder of the trial until reward was delivered for successful performance (red dots). Figure 3B shows overall mean ± *SEM* firing rates for all RS frontal cortical cells recorded in Layer 2/3 (n = 54) and Layer 5 (n = 40) that showed significantly increased firing during start ring presentation. Mean firing rates were significantly elevated in both Layer 2/3 and Layer 5 after the start ring presentation relative to baseline firing rates measured 600 msec before image appearance; Layer 2/3 StartR, 7.60 ± 0.73 Hz versus baseline, 4.44 ± 0.83 Hz, $F(4,3265) = 6.65$, $p < .001$; Layer 5 StartR, 7.72 ± 0.82 Hz versus baseline, 4.80 ± 0.47 Hz, $F(4, 3033) = 5.02$, $p < .001$. Comparison of start ring induced increased (mean) firing rates of Layer 2/3 versus Layer 5 neurons (i.e., sites 2a–d vs. 5 a–d in Figure 3B) revealed no significant differences.

Frontal Cortical Cell Firing: Go Target Presentation

The raster displays and PEHs in Figure 4A show the phasic firing of two RS frontal cortical neurons recorded at MEA recording site 2a in Layer 2/3 (upper) and at site 5b in Layer 5 (lower) to go target presentation during performance of the go/no-go task. The red dots in the raster displays denote the time of occurrence of the *go response* after go target presentation. Both cells showed a marked increase in firing after presentation of the go target image with clear differences in the patterns of discharge, which decreased to baseline firing rates in both neurons within 0.5 sec (Figure 4A). Figure 4B shows a CCH indicating the probability of the Layer 5 cell firing (Figure 4A, lower) within ±10 msec of spike

occurrences recorded simultaneously in the Layer 2/3 cell (Figure 4A, upper), assessed selectively over the ±2.0-sec PEH period and summed over all go target trials in the session. The large increase and relatively restricted firing probability (±2.0 msec) of the Layer 5 cell relative to Layer 2/3 cell spike occurrences is suggestive of task-related synchronization between layers for cells with a straight line vertical orientation (2a and 5b) on the MEA (diagram in Figure 4).

Figure 5A and B shows the mean ± *SEM* firing rates for all frontal cortical RS neurons recorded in Layer 2/3 and Layer 5 in response to go target presentation during the task, displayed according to recording sites with the same straight line vertical orientations (Figure 5A: 2a–d and 5a–b; Figure 5B: 2c–d and5c–d) on theMEA. The mean firing rate of all Layer 2/3 cells ($n = 51$) recorded at probe sites 2ab and 2cd showed an increase and significant transient firing peak immediately after (+0.25–0.50 sec) go target presentation with respect to the prior baseline (−2.0 sec) rate; Layer 2/3 GoT, 9.92 ± 1.12 Hz versus baseline, 4.43 ± 0.22 Hz, $F(4, 2360) = 5.90$, $p < .001$. Layer 5 cells ($n = 53$) in both lower MEA recording pad locations (5ab and 5cd) also showed significantly increased peaks in mean firing rate to go target presentation relative to baseline mean rate; Layer 5 GoT, 6.91 ± 0.78 Hz versus baseline, 4.32 ± 0.16 Hz, $F(4, 2486) = 4.68$, $p < .001$. The asterisks in Figure 5A and B indicate significant differences between peak mean firing rates at Layer 2/3 MEA recording sites versus peak rates at Layer 5 sites with respect to both vertical orientations; ab sites: Layer 2/3, 10.83 ± 1.25 Hz versus Layer 5, 7.09 ± 0.89, $F(1, 2486) = 4.61$, $p < .01$; cd sites: Layer 2/3, 9.01 ± 1.31 Hz versus Layer 5, 6.25 ± 1.31, $F(1, 2486) = 4.44$, $p < .01$. To examine synchronization of FCx cell firing between layers, mean ± *SEM* CCHs shown in Figure 5C were constructed for cell pairs recorded at sites 2ab–5ab and 2cd–5cd for ±2.0 sec relative to go target presentation (0 sec, Figure 5A and B). CCHs showed marked synchronized firing in terms of increased mean ± *SEM* firing probability, $F(1, 1783) = 19.49$, $p < .001$, for cell pairs recorded in both layers at parallel straight line vertical locations (2ab–5ab and 2cd–5cd) on the MEA (Figure 5C).

Figure 5C suggests that laminar processing may be specific to restricted columnar-like projections between cells in Layer 2/3 and Layer 5 during performance of go target trials (de Kock et al., 2007; Derdikman et al., 2006; Zhang & Alloway, 2006; Krupa, West, Shuler, Laubach, & Nicolelis, 2004). To compare firing patterns across such putative cortical minicolumns, mean ± *SEM* CCHs of spike activity during go target presentation from pairs of cells simultaneously recorded with straight line (2ab–5ab, 2cd–5cd) versus opposite (2ab–5cd, 2cd–5ab) vertical orientations on the MEA were compared. Figure 5D shows the mean ± *SEM* CCHs for cell pairs with the straight line vertical orientations (2ab–5ab, red bars) for cells in Layer 2/3 ($n = 35$) and Layer 5 ($n = 41$) versus CCHs for the same Layer 2/3 cells (2ab) paired with Layer 5 cells ($n = 44$) recorded simultaneously at sites with the opposite (5cd, blue bars) vertical orientation. It is clear that pairs of Layer 2/3 and Layer 5 cells recorded from MEA pads with the same (straight line) vertical orientation showed more synchronized firing in terms of higher firing probabilities than pairs recorded from sites on the MEA with the opposite vertical orientations (i.e., nonvertical orientations), $F(1, 3356) = 31.2$, $p < .001$. However, it is also apparent from Figure 5D that cells recorded at sites 5cd showed no significant correlation with the spikes of cells recorded at locations 2ab during go target presentation while the animals performed the task. Importantly, this lack of synchronized firing between 2ab and 5cd sites (blue bars in Figure 5D) was related specifically to the different vertical orientations of the cell pairs and not the inability of cells recorded at 5cd sites to exhibit synchronized firing because the CCHs shown in Figure 5C for MEA recording sites 2cd–5cd included some of the Layer 5 cells tested in Figure 5D.

Frontal Cortical Cell Firing: Go Response

Neuronal activity in prefrontal cortical cells before the movement initiation has been hypothesized to be related to movement planning and preparation (Tsujimoto, Genovesio, & Wise, 2008; Genovesio, Brasted, & Wise, 2006; Hoshi & Tanji, 2000; Boussaoud & Wise, 1993). Figure 6A shows two FCx cells recorded in Layer 2/3 (MEA recording site 2c) and Layer 5 (probe site 5d) with enhanced firing associated with limb movement before and during placement of the cursor in the image (red line at 0 sec) after go target presentation (red dots in the raster). In contrast to the Layer 2/3 neuron, the Layer 5 cell exhibited an increase in firing before and after completion of the go response (red line at 0 sec). Figure 6B shows the different mean ± *SEM* firing patterns of all cells recorded at MEA recording sites 2a–d (upper graph) in Layer 2/3 ($n = 38$) and sites 5a–d (lower graph) in Layer 5 ($n = 43$) during the time epoch between go target presentation and occurrence of the go response (red line at 0 sec). Layer 2/3 cells showed a significant peak increases in firing 0.5 sec before the go response relative to mean baseline rate prior to go target presentation; Layer 2/3 GoR, 7.69 ± 1.28 Hz versus baseline, 4.58 ± 0.27 Hz, $F(4, 1688) = 4.54$, $p < .001$. Neurons recorded in Layer 5 showed a significant mean firing peak 0.8 sec before the go response (Layer 5 GoR, 7.29 ± 0.8 Hz vs. baseline GoR, 4.97 ± 0.22 Hz), $F(4, 2749) = 4.52$, $p < .001$, $n = 43$ cells, followed by a brief decrease in firing rate at the go response (red line 0.0 sec) then a rapid secondary increase to a secondary peak 0.5 sec after the response (Layer 5 post-GoR, 7.52 ± 0.70 Hz), $F(4, 2749) = 5.13$, $p < .001$. The firing probability (mean ± *SEM*) between pairs of cells in Layer 2/3 and Layer 5 during the go response is shown in the CCHs in Figure 6C. Synchronized firing between pairs of cells with the same vertical orientation ($n = 21$) on the MEA (2ab–5ab, 2cd–5cd) was much greater than for cell pairs ($n = 12$) with the opposite (2ab–5cd, 2cd–5ab) vertical orientation, $F(1, 2117) = 27.7$, $p < .001$.

FCx Cell Firing: No-Go Stimulus Presentation

Figure 7A shows FCx activity from a Layer 2/3 cell and a Layer 5 cell in response to presentation of the no-go stimulus image during single sessions of the go/no-go task. The differential firing patterns shown in the raster and PEH displays are similar to that shown for go target presentation (Figure 4A). Figure 7B depicts the mean ± *SEM* firing rates of all recorded Layer 2/3 ($n = 41$) and Layer 5 ($n = 32$) cells to presentation of the no-go stimulus. Layer 2/3 cells exhibited a pronounced peak in mean firing rate immediately after (+0.25 sec) presentation (0 sec red line) relative to the prior baseline rate; Layer 2/3 No-goS, 9.13 ± 1.14 Hz versus baseline no-go stimulus, 4.04 ± 0.21 Hz, $F(4, 1544) = 5.14$, $p < .001$. The mean firing increase of Layer 5 cells to presentation of the no-go stimulus was also significant (Layer 5 No-goS: 6.07 ± 1.21 Hz), $F(4, 1338) = 3.94$, $p < .01$; however, the peak was much smaller (Figure 7B lower) than the Layer 2/3 increase, $F(1, 2883) = 7.53$, $p < .01$. Figure 7C shows mean ± *SEM* CCHs for pairs of Layer 2/3 and Layer 5 cells with the same (2ab–5ab or 2cd–5cd) and opposite (2ab–5cd or 2cd–5ab) MEA site vertical orientations during (±2.0 sec) no-go stimulus presentation. Synchronous firing was only observed in pairs of cells with the same vertical orientations (2ab–5ab or 2cd–5cd) as previously shown for other task-related events (Figures 5D and 6C). After the no-go stimulus presentation, the mean ± *SEM* activity of the FCx cells shown in Figure 7B was assessed for the remaining 3.5 sec of the no-go timeout interval. During this interval, behavioral responses were suppressed, and the juice reward presented when the interval timed out (red line at 5.0 sec; Figure 7A). Both Layer 2/3 cells and Layer 5 cells showed erratic smaller positive/negative fluctuations in mean firing rate for the remainder of the interval; however, there were no significant changes from baseline firing rate or differences in mean rate between layers (Figure 7B, lower) during this 3.5-sec period.

FS Frontal Cortical Cells

Another class of FCx neurons shown to participate in laminar processing is FS cells or interneurons that populate both Layer 2/3 and Layer 5 (Weiler et al., 2008; Derdikman et al., 2006; Zhang & Alloway, 2006; Shepherd & Svoboda, 2005; Krupa et al., 2004; Mountcastle, 2003). Figure 8 shows that FS cells recorded in Layer 2/3 (upper, $n = 22$) and in Layer 5 (lower, $n = 39$) during start ring presentation exhibited much higher baseline (−2.0 sec) mean firing rates (Layer 2/3 FS, 8.13 ± 0.37 Hz; Layer 5 FS, 15.12 ± 0.29 Hz) than RS neurons (Figures 3–7). The FS neurons recorded in both layers showed significant increases in mean ± *SEM* firing rate within 1.0 sec of start ring presentation (Layer 2/3 FS-SR, 12.47 ± 2.11 Hz vs. baseline FS, 8.13 ± 0.37 Hz, $F(4, 3388) = 4.09$, $p < .01$; Layer 5 peak FS-SR, 21.47 ± 2.83 Hz. versus baseline FS, 14.62 ± 0.29 Hz, $F(4, 3014) = 5.19$, $p < .001$) in spite of high baseline firing rates (Figure 8B). CCHs of mean ± *SEM* firing probabilities for pairs of FS cells detected on the same (2ab–5ab or 2cd–5cd) or opposite (2ab–5cd or 2cd–5ab) vertical sites on the MEA showed exceedingly high synchronized firing for cell pairs with the same vertical orientation versus pairs of cells with the opposite orientation, $F(1, 1916) = 31.1$, $p<.001$,onthe MEA (Figure 8C).

DISCUSSION

The current study examined the activity of neurons recorded simultaneously in the supragranular (Layer 2/3) and infragranular (Layer 5) lamina of FCx in NHPs performing a simple go/no-go task. The findings provide unique assessments of the neural correlates of sensory processing during the task and firing associated with motor responses to task-specific signals of RS cells in these two layers in terms of specificity and degree of event-related activation as well as synchronization of cell firing across layers.

Layer-specific Frontal Cortical Activity Recorded with Conformal Electrodes

Implementation of the newly applied MEA technology described here (Hampson, Coates, et al., 2004; Moxon et al., 2004; Burmeister, Moxon, & Gerhardt, 2000) allowed simultaneous recording from neurons at two different anatomically and physiologically distinct recording sites in the sensorimotor areas of FCx. The conformal design of the MEA allowed identification and designation of activity within a dual laminar arrangement of orthogonal electrode recording sites separated by 1350 μm, the precise distance between Layer 2/3 and Layer 5 in the FCx Arcuate sulcus (Figure 1). This recording arrangement allowed unique comparisons of the simultaneous activity of cells from (i) each separate cortical layer and (ii) within the same layer but at adjacent physically separate locations on the MEA (Figure 2). The differential firing to task-related events of identified FCx cells in both Layer 2/3 and Layer 5 is described in detail in Figures 3–7 in terms of individual and mean discharge patterns of simultaneously recorded neurons in each layer during either go or no-go trials.

Differential Involvement of Neurons in Layer 2/3 and Layer 5 in Task-related Events

Figure 9 presents a composite firing profile of the average firing pattern across all cells in each cell layer recorded continuously over the entire duration of either a go or a no-go trial. The discharge patterns of the FCx cell populations summed across all MEA recording sites in each cortical layer show that most RS (and FS; Figure 8) cells increased firing significantly during the start ring which initiated the trial. However, Figure 9 shows that subsequent average firing rate in the overall cell population of Layer 2/3 cells during go and no-go target presentations (Figures 3–7) was consistently more pronounced than the increase in firing in the Layer 5 cell population, which was more increased after the go response, suggesting that stimulus events depicting trial information were a primary factor differentiating firing between layers. Presumably, during presentation of task stimuli (i.e., start ring or go/no-go target images), sensory information (visual spatial, color, shape, and

brightness) was processed and conveyed to neurons in Layer 2/3 via ascending fibers from visual cortex (Weiler et al., 2008; Ferrera, Cohen, & Lee, 1999; Kritzer & Goldman-Rakic, 1995). In contrast, Figure 9 also shows that the average firing rate during the go response phase of the task was distinctly higher in Layer 5 cells (Figure 9, Response); therefore, layer-specific activity was detected via the unique conformal design of the MEA, which allowed simultaneous recordings of differential firing patterns of cells from both layers.

Firing of FCx Layer 2/3 cells has been suggested to reflect processing of information relevant to the planning of behavioral/motor acts (de Kock & Sakmann, 2009; Nakayama, Yamagata, Tanji, & Hoshi, 2008; Derdikman et al., 2006). The tendency for Layer 2/3 neurons to fire less during the well-trained go response indicates reduced involvement in actual execution of motor acts (i.e., limb movement) compared with Layer 5 cells (Figures 7 and 9). The propensity for Layer 2/3 cells to show more robust firing during go and no-go target presentations could reflect a number of factors such as more extensive horizontal connections allowing integration over a larger part of the receptive field (Gilbert & Wiesel, 1989), integration of spatial location and color information (Ferrera et al., 1999; Rao, Rainer, & Miller, 1997), or sensory motor processing (Fuster, 2001). However, because both trial-specific image presentations (go target and no-go stimuli) produced similar firing differences between layers (Figures 5, 7, and 9), the differential activation could not be due to ensuing task contingencies involving limb movement (go target/response trials) or, alternatively, the suppression of such movements (no-go stimulus/timeout trials).

Columnar Processing of Task-relevant Events between Cortical Layers

In addition to the differential laminar processing of sensory stimuli in Layer 2/3 and Layer 5, a difference was also demonstrated with respect to synchronized firing of pairs FCx RS (and FS) cells with different vertical orientations “across layers” during the same task-related events. This was demonstrated explicitly in CCHs by marked differences in mean firing probabilities of pairs of Layer 2/3 and Layer 5 cells recorded from the same or opposite vertically oriented recording sites on the conformal MEA (Figures 3–8). Figure 10 shows this type of comparison combined for all task-related events to illustrate the fact that pairs of Layer 2/3 and Layer 5 cells that were not aligned in the same vertical orientation across layers (defined by the 40-μm lateral separation of recording sites on the MEA; Figure 1) showed no synchronous firing (noncolumnar), whereas Layer 2/3 and Layer 5 cells recorded at sites with the same vertical orientation (columnar) exhibited a high degree of synchronous firing. Two important factors shown in Figure 10 (columnar) indicate that cells in Layer 5 with the same vertical orientation were synchronized to the firing of Layer 2/3 cells with (i) significantly increased likelihood of discharge ≥1.0 msec relative to each spike occurrence of Layer 2/3 cells and (ii) slightly suppressed firing below background levels at ±1.0 to 2.0 msec indicative of refraction in the some cells. Figure 10 also shows that firing was clustered at 0.0 ± 1.0 msec, indicating possible synchronized common inputs to cells in Layer 2/3 and Layer 5 to activate the column from other sources. These features were not present in mean CCHs of Layer 5 cell activity recorded from opposite vertical recording sites (Figure 10, noncolumnar), although some of the same Layer 5 cells showed synchronized firing with different Layer 2/3 cells recorded at MEA sites with the same vertical orientation—just at a different parallel location (i.e., 2ab vs. 2cd) on the MEA. This result agrees with prior findings in which firing properties in neighboring electrodes within FCx varied somewhat abruptly as would be expected from lateral inhibitory influences in a columnar processing neural substrate (Mountcastle, 1997; Schlaug, Schleicher, & Zilles, 1995) and provides evidence for a functional anatomic substrate made up of cortical minicolumns (Mountcastle, 2003; Kritzer & Goldman-Rakic, 1995; Schlaug et al., 1995). The findings are also supported by prior (Buxhoeveden & Casanova, 2002; Mountcastle, 1997; Peters & Sethares, 1991) and recent (Casanova, Trippe, Tillquist, & Switala, 2009)

estimates of the size of cortical minicolumns in NHPs as being less than 40 microns in diameter.

Frontal Cortical Microcircuitry and Sensorimotor Processing

Previous anatomical studies in the pFC of primates (Elston et al., 2006; Rempel-Clower & Barbas, 2000; Melchitzky et al., 1998; Kritzer & Goldman-Rakic, 1995) have provided valuable insight into the intrinsic "laminar" circuit organization of cortical layers, with pyramidal cells targeting long-range horizontal connections to columns with similar functional properties (Mountcastle, 1997; Schlaug et al., 1995). In agreement with previous studies of cortical columnar organization (Weiler et al., 2008; Derdikman et al., 2006; Zhang & Alloway, 2006; Krupa et al., 2004; Jung et al., 1998), functional evidence is provided here for both *laminar processing* across different cortical layers (Figures 3–9) and parallel *columnar processing* (Figures 3–8, 10) in subregions, consistent with a highly complex but organized frontal cortical microcircuitry.

Local circuits within and between layers of the cortical column in the FCx have been shown to be critically involved in mediating goal oriented behavior because such circuits receive and integrate convergent sensory inputs (Layer 2/3) and motor systems (Layer 5) for movement planning and reaching (Weiler et al., 2008; Hoshi & Tanji, 2006; Shepherd & Svoboda, 2005; Shipp, 2005; Callaway, 1998; Hirsch, 1995). The coordinated output from infragranular Layer 5 cells (which receive convergent excitatory inputs from Layer 2/3 pyramidal cells as shown in Figures 3–7) presumably transmit signals to other cortical and subcortical targets (Nakayama et al., 2008; Derdikman et al., 2006; Zhang & Alloway, 2006; Zikopoulos & Barbas, 2006; Ohbayashi, Ohki, & Miyashita, 2003), generating planned motor actions and movements (Weiler et al., 2008; Takeda et al., 2004).

The current results demonstrate many of functional "operations" described above in which frontal cortical neurons in both the supragranular and the infragranular layers differentially encoded sensory stimuli relevant to performance of a simple go/no-go task. In addition, firing to task-related events was shown to be encoded between layers by synchronized firing of cell pairs comprising apparent functional "minicolumns" connecting the supragranular and the infragranular layers. This assessment was made possible by use of conformal MEAs designed to sample frontal cortical activity in a manner that would reveal the demonstrated functional columnar organization of FCx. The results provide new insight into the manner in which underlying frontal cortical microcircuitry integrates convergent sensory and motor signals from other brain regions to select and control task-related behavioral response tendencies in primate brain.

Acknowledgments

The authors thank Joshua Long, Joseph Noto, Michael Todd, and Santos Ramirez at the Wake Forest University Medical School and Peter Huettl at the University of Kentucky for their assistance on this Project. This work was supported by NSF EEC-0310723, DARPA N66020, and NIH grants DA06634, DA023573, and DA026487 to S. A. D.

REFERENCES

Andersen RA, Buneo CA. Sensorimotor integration in posterior parietal cortex. Advances in Neurology. 2003; 93:159–177. [PubMed: 12894407]

Barbas H, Pandya DN. Architecture and frontal cortical connections of the premotor cortex (area 6) in the rhesus monkey. Journal of Comparative Neurology. 1987; 256:211–228. [PubMed: 3558879]

Barbas H, Pandya DN. Architecture and intrinsic connections of the prefrontal cortex in the rhesus monkey. Journal of Comparative Neurology. 1989; 286:353–375. [PubMed: 2768563]

Boussaoud D, Wise SP. Primate frontal cortex: Effects of stimulus and movement. Experimental Brain Research. 1993; 95:28–40.

Burmeister JJ, Moxon K, Gerhardt GA. Ceramic-based multisite microelectrodes for electrochemical recordings. Analytical Chemistry. 2000; 72:187–192. [PubMed: 10655652]

Burmeister JJ, Pomerleau F, Huettl P, Gash CR, Werner CE, Bruno JP, et al. Ceramic-based multisite microelectrode arrays for simultaneous measures of choline and acetylcholine in CNS. Biosensors & Bioelectronics. 2008; 23:1382–1389. [PubMed: 18243683]

Buxhoeveden DP, Casanova MF. The minicolumn hypothesis in neuroscience. Brain. 2002; 125:935–951. [PubMed: 11960884]

Callaway EM. Local circuits in primary visual cortex of the macaque monkey. Annual Review of Neuroscience. 1998; 21:47–74.

Caminiti R, Ferraina S, Mayer AB. Visuomotor transformations: Early cortical mechanisms of reaching. Current Opinion in Neurobiology. 1998; 8:753–761. [PubMed: 9914239]

Casanova MF, Trippe J, Tillquist C, Switala AE. Morphometric variability of minicolumns in the striate cortex of *Homo sapiens*, *Macaca mulatta* and *Pan troglodytes*. Journal of Anatomy. 2009; 214:226–234. [PubMed: 19207984]

Constantinidis C, Franowicz MN, Goldman-Rakic PS. Coding specificity in cortical microcircuits: A multiple-electrode analysis of primate prefrontal cortex. Journal of Neuroscience. 2001; 21:3646–3655. [PubMed: 11331394]

Constantinidis C, Williams GV, Goldman-Rakic PS. A role for inhibition in shaping the temporal flow of information in prefrontal cortex. Nature Neuroscience. 2002; 5:175–180.

Crammond DJ, Kalaska JF. Modulation of preparatory neuronal activity in dorsal premotor cortex due to stimulus-response compatibility. Journal of Neurophysiology. 1994; 71:1281–1284. [PubMed: 8201421]

de Kock CP, Bruno RM, Spors H, Sakmann B. Layer- and cell-type-specific suprathreshold stimulus representation in rat primary somatosensory cortex. Journal of Physiology. 2007; 581:139–154. [PubMed: 17317752]

de Kock CP, Sakmann B. Spiking in primary somatosensory cortex during natural whisking in awake head-restrained rats is cell-type specific. Proceedings of the National Academy of Sciences, U.S.A. 2009; 106:16446–16450.

Derdikman D, Yu C, Haidarliu S, Bagdasarian K, Arieli A, Ahissar E. Layer-specific touch-dependent facilitation and depression in the somatosensory cortex during active whisking. Journal of Neuroscience. 2006; 26:9538–9547. [PubMed: 16971538]

di Pellegrino G, Wise SP. Visuospatial versus visuomotor activity in the premotor and prefrontal cortex of a primate. Journal of Neuroscience. 1993; 13:1227–1243. [PubMed: 8441009]

Dombrowski SM, Hilgetag CC, Barbas H. Quantitative architecture distinguishes prefrontal cortical systems in the rhesus monkey. Cerebral Cortex. 2001; 11:975–988. [PubMed: 11549620]

Douglas RJ, Martin KA. Neuronal circuits of the neocortex. Annual Review of Neuroscience. 2004; 27:419–451.

Elston GN, Benavides-Piccione R, Elston A, Zietsch B, Defelipe J, Manger P, et al. Specializations of the granular prefrontal cortex of primates: Implications for cognitive processing. Anatomical Record, Part A, Discoveries in Molecular, Cellular, and Evolutionary Biology. 2006; 288A:26–35.

Fadiga L, Craighero L. New insights on sensorimotor integration: From hand action to speech perception. Brain and Cognition. 2003; 53:514–524. [PubMed: 14642302]

Ferrera VP, Cohen JK, Lee BB. Activity of prefrontal neurons during location and color delayed matching tasks. NeuroReport. 1999; 10:1315–1322. [PubMed: 10363946]

Funahashi S, Inoue M. Neural interactions related to working memory processes in the primate prefrontal cortex revealed by cross-correlation analysis. Cerebral Cortex. 2000; 10:535–551. [PubMed: 10859132]

Fuster JM. The prefrontal cortex—An update: Time is of the essence. Neuron. 2001; 30:319–333. [PubMed: 11394996]

Genovesio A, Brasted PJ, Wise SP. Representation of future and previous spatial goals by separate neural populations in prefrontal cortex. Journal of Neuroscience. 2006; 26:7305–7316. [PubMed: 16822988]

Gilbert CD, Wiesel TN. Columnar specificity of intrinsic horizontal and corticocortical connections in cat visual cortex. Journal of Neuroscience. 1989; 9:2432–2442. [PubMed: 2746337]

González-Burgos G, Barrionuevo G, Lewis DA. Horizontal synaptic connections in monkey prefrontal cortex: An in vitro electrophysiological study. Cerebral Cortex. 2000; 10:82–92. [PubMed: 10639398]

Hampson, RE.; Coates, TD., Jr; Gerhardt, GA.; Deadwyler, SA. Ceramic-based microelectrode neuronal recordings in the rat and monkey. Proceedings of the Annual International Conference of the IEEE Engineering in Medicine and Biology Society; 2004. p. 3700-3703.

Hampson RE, Pons TP, Stanford TR, Deadwyler SA. Categorization in the monkey hippocampus: A possible mechanism for encoding information into memory. Proceedings of the National Academy of Sciences, U.S.A. 2004; 101:3184–3189.

Hirsch JA. Synaptic integration in layer 4 of the ferret striate cortex. Journal of Physiology (London). 1995; 483:183–199. [PubMed: 7776231]

Hoshi E, Tanji J. Integration of target and body-part information in the premotor cortex when planning action. Nature. 2000; 408:466–470. [PubMed: 11100727]

Jung MW, Qin Y, McNaughton BL, Barnes CA. Firing characteristics of deep layer neurons in prefrontal cortex in rats performing spatial working memory tasks. Cerebral Cortex. 1998; 8:437–450. [PubMed: 9722087]

Kritzer MF, Goldman-Rakic PS. Intrinsic circuit organization of the major layers and sublayers of the dorsolateral prefrontal cortex in the rhesus monkey. Journal of Comparative Neurology. 1995; 359:131–143. [PubMed: 8557842]

Krupa DJ, West MC, Shuler MG, Laubach M, Nicolelis MA. Layer-specific somatosensory cortical activation during active tactile discrimination. Science. 2004; 304:1989–1992. [PubMed: 15218154]

Kubota K, Komatsu H. Neuron activities of monkey prefrontal cortex during the learning of visual discrimination tasks with GO/NO-GO performances. Neuroscience Research. 1985; 3:106–129. [PubMed: 3837861]

Lebedev MA, Messinger A, Kralik JD, Wise SP. Representation of attended versus remembered locations in prefrontal cortex. PLoS Biology. 2002; 2:e365.. Epub 2004 Oct 26. [PubMed: 15510225]

Lorente de No, R. Cerebral cortex: Architecture, intracortical connections, motor projections. In: Fulton, JF., editor. Physiology of the nervous system. Vol. 3rd ed.. Oxford: Oxford University Press; 1949. p. 288-330.

Melchitzky DS, Sesack SR, Pucak ML, Lewis DA. Synaptic targets of pyramidal neurons providing intrinsic horizontal connections in monkey prefrontal cortex. Journal of Comparative Neurology. 1998; 390:211–224. [PubMed: 9453665]

Miller EK, Cohen JD. An integrative theory of prefrontal cortex function. Annual Review of Neuroscience. 2001; 24:167–202.

Mountcastle VB. The columnar organization of the neocortex. Brain. 1997; 120:701–722. [PubMed: 9153131]

Mountcastle VB. Introduction. Cerebral Cortex. 2003; 13:2–4. [PubMed: 12466209]

Moxon KA, Leiser SC, Gerhardt GA, Barbee KA, Chapin JK. Ceramic-based multisite electrode arrays for chronic single-neuron recording. IEEE Transactions on Biomedical Engineering. 2004; 51:647–656. [PubMed: 15072219]

Mushiake H, Inase M, Tanji J. Neuronal activity in the primate premotor, supplementary, and precentral motor cortex during visually guided and internally determined sequential movements. Journal of Neurophysiology. 1991; 66:705–718. [PubMed: 1753282]

Nakayama Y, Yamagata T, Tanji J, Hoshi E. Transformation of a virtual action plan into a motor plan in the premotor cortex. Journal of Neuroscience. 2008; 28:10287–10297. [PubMed: 18842888]

Ohbayashi M, Ohki K, Miyashita Y. Conversion of working memory to motor sequence in the monkey premotor cortex. Science. 2003; 301:233–236. [PubMed: 12855814]

Opris I, Barborica A, Ferrera VP. Microstimulation of dorsolateral prefrontal cortex biases saccade target selection. Journal of Cognitive Neuroscience. 2005; 17:893–904. [PubMed: 15969908]

Opris I, Bruce CJ. Neural circuitry of judgment and decision mechanisms. Brain Research Reviews. 2005; 48:509–528. [PubMed: 15914255]

Opris I, Hampson RE, Deadwyler SA. The encoding of cocaine vs. natural rewards in the striatum of nohuman primates: Categories with different activations. Neuroscience. 2009; 163:40–54. [PubMed: 19501630]

Passingham, RE. The frontal lobes and voluntary action. Oxford: Oxford UP; 1993.

Paxinos, G.; Huang, XF.; Toga, AW. The rhesus monkey brain in stereotaxic coordinates. San Diego: Academic Press; 2000.

Peters A, Sethares C. Organization of pyramidal neurons in area 17 of monkey visual cortex. Journal of Comparative Neurology. 1991; 306:1–23. [PubMed: 1710236]

Rao SC, Rainer G, Miller EK. Integration of what and where in the primate prefrontal cortex. Science. 1997; 276:821–824. [PubMed: 9115211]

Rao SG, Williams GV, Goldman-Rakic PS. Isodirectional tuning of adjacent interneurons and pyramidal cells during working memory: Evidence for microcolumnar organization of PFC. Journal of Neurophysiology. 1999; 81:1903–1916. [PubMed: 10200225]

Rempel-Clower NL, Barbas H. The laminar pattern of connections between prefrontal and anterior temporal cortices in the rhesus monkey is related to cortical structure and function. Cerebral Cortex. 2000; 10:851–865. [PubMed: 10982746]

Rizzolatti G, Gentilucci M, Fogassi L, Luppino G, Matelli M, Ponzoni-Maggi S. Neurons related to goal-directed motor acts in inferior area 6 of the macaque monkey. Experimental Brain Research. 1987; 67:220–224.

Sakurai Y, Takahashi S. Dynamic synchrony of firing in the monkey prefrontal cortex during working-memory tasks. Journal of Neuroscience. 2006; 26:10141–10153. [PubMed: 17021170]

Schlaug G, Schleicher A, Zilles K. Quantitative analysis of the columnar arrangement of neurons in the human cingulated cortex. Journal of Comparative Neurology. 1995; 351:441–452. [PubMed: 7706552]

Schwartz AB, Moran DW, Reina GA. Differential representation of perception and action in the frontal cortex. Science. 2004; 303:380–383. [PubMed: 14726593]

Shepherd GMG, Svoboda K. Laminar and columnar organization of ascending excitatory projections to layer 2/3 pyramidal neurons in rat barrel cortex. Journal of Neuroscience. 2005; 25:5670–5679. [PubMed: 15958733]

Shipp S. The importance of being agranular: A comparative account of visual and motor cortex. Philosophical Transactions of the Royal Society of London, Series B, Biological Sciences. 2005; 360:797–814.

Takeda M, Nambu A, Hatanaka N, Tachibana Y, Miyachi S, Taira M, et al. Organization of prefrontal outflow toward frontal motor-related areas in macaque monkeys. European Journal of Neuroscience. 2004; 19:3328–3342. [PubMed: 15217388]

Takeda SI, Funahashi S. Reward-period activity in primate dorsolateral prefrontal and orbitofrontal neurons is affected by reward schedules. Journal of Cognitive Neuroscience. 2006; 18:212–226. [PubMed: 16494682]

Tsujimoto S, Genovesio A, Wise SP. Transient neuronal correlations underlying goal selection and maintenance in prefrontal cortex. Cerebral Cortex. 2008; 18:2748–2761. [PubMed: 18359779]

Weiler N, Wood L, Yu J, Solla SA, Shepherd GM. Top-down laminar organization of the excitatory network in motor cortex. Nature Neuroscience. 2008; 11:360–366.

Wise SP. The primate premotor cortex: Past, present, and preparatory. Annual Review of Neuroscience. 1985; 8:1–19.

Yoshimura Y, Dantzker JL, Callaway EM. Excitatory cortical neurons form fine-scale functional networks. Nature. 2005; 433:868–873. [PubMed: 15729343]

Zhang M, Alloway KD. Intercolumnar synchronization of neuronal activity in rat barrel cortex during patterned air jet stimulation: A laminar analysis. Experimental Brain Research. 2006; 169:311–325.

Zikopoulos B, Barbas H. Prefrontal projections to the thalamic reticular nucleus form a unique circuit for attentional mechanisms. Journal of Neuroscience. 2006; 26:7348–7361. [PubMed: 16837581]

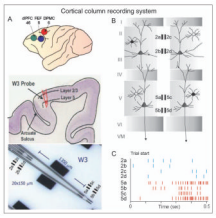

Figure 1.

FCx recording sites with conformal ceramic MEA. (A) Illustration of NHP brain (*upper*) showing frontal and prefrontal cortical recording locations (Areas 46, 8, 6), cross-section of arcuate sulcus (*middle*) showing location of Layer 2/3 and Layer 5 with electrode track and close up of W3-ceramic MEA (*lower*) with dimensions of four separated (1350 μm) recording sites (Area: 20 × 150 μm/site, 40 μm separation between sites) designated for each layer (2a–d, 5a–d). dlPFC = dorsolateral pFC; dPMC = dorsal premotor cortex. (B) Diagram showing arrangement of ceramic MEA recording sites relative to orientation of pyramidal cell bodies and dendrites in Layer 2/3 and Layer 5 in arcuate sulcus. Filled rectangles depict grouping of recording sites (2a–d, 5a–d) on ceramic MEA shown in panel B within each layer. (C) Illustration of FCx multineuron activity recorded simultaneously in each layer during a single go/no-go trial. Tick marks depict occurrence of extracellular recorded action potentials (spikes) over time (sec) at each of the indicated electrode recording sites.

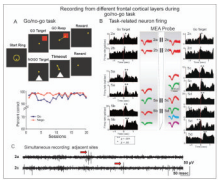

Figure 2.

Task-related FCx neuron activity recorded with ceramic MEA. (A) Diagram of go/no-go task shows images to which animals responded in different task phases on each type of trial. go Resp = selection of go target; Timeout = 5.0 sec delay interval on *no-go* trial. Below: Mean performance for go target and no-go stimulus trials for all animals (n = 3), indicating that nearly perfect performance during stage of testing in which neuronal activity was acquired. (B) Display shows activity recorded during a single go/no-go session from 14 individual FCx neurons (superimposed waveforms, calibration = 1 msec, 150 μV) distributed in Layer 2/3 and Layer 5 from an animal during go/no-go task performance. Neurons were detected and electronically isolated at the individual recording sites on the ceramic MEA probe diagram with more than one neuron (indicated by differences in waveform) isolated from some recording sites. PEHs next to waveforms show average firing rate (Hz) of the same neurons during go target presentations (red line 0.0 sec) within the go/no-go session. Asterisks in PEHs indicate significant increases in peak firing over baseline rates before go target presentation. (C) Strip chart of real-time simultaneous records from recording sites 2a–c separated by 40 μm on ceramic MEA probe shows that the same signals, including extracellular action potentials (arrows), were not routinely detected on both sites despite proximity. Continuous waveforms were amplified 10,000×, band-pass filtered from 250 to 8000 Hz, and digitized at 40 kHz. Scale bar: 50 msec, 50 mV (before amplification).

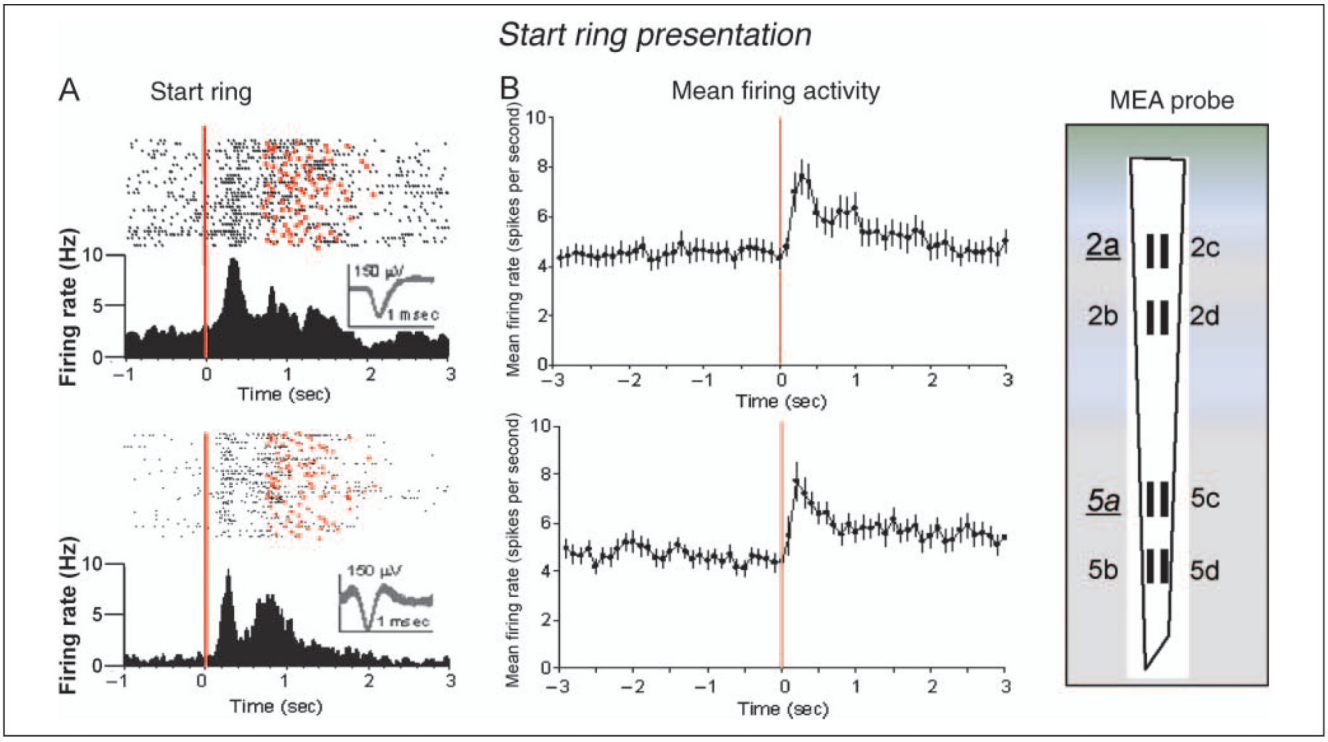

Figure 3.

Task-related FCx neuron firing: start ring presentation. (A) Single trial raster displays and PEHs illustrate firing patterns (black dots) of two RS FCx pyramidal cells (waveform calibration = 1.0 msec, 150 µV) recorded from Layer 2/3 (upper) or Layer 5 (lower) at the indicated MEA probe recording sites (2a and 5a) for 1.0 sec before and 3.0 sec after start ring presentation (0.0 sec red line). Trial completion via either reward delivery or occurrence of error response indicated by red dots in the raster displays. (B) Mean ± *SEM* firing rates for all RS FCx cells recorded in Layer 2/3 (upper) at MEA sites 2a–d (n = 54) or Layer 5 (below) at MEA sites 5a–d (n = 40) for ±3.0 sec during start ring presentation (0.0 sec, red line) summed over all trials (mean rates = 100-msec bins).

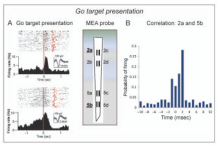

Figure 4.

Task-related FCx neuron firing: go target presentation. (A) Single session PEHs and raster displays for two RS FCx cells recorded in Layer 2/3 (upper: MEA probe site 2a) or Layer 5 (lower: MEA site 5b) in response to go target presentation (red line, 0 sec). Red dots in raster displays indicate occurrence of go response on each trial. Insets: superimposed waveforms from each neuron (calibration = 1.0 msec, 150 μV). (B) CCH of cell pairs at different sites showing mean (*SEM*) probability of firing (ratio of extracellular spike occurrences) of Layer 5 RS FCx cells recorded at MEA site 5b (lower raster and PEH in panel A) within ±10.0 msec of individual spike occurrences from the Layer 2/3 RS FCx cell (0 msec in CCH) recorded at site 2a (upper raster and PEH). Firing synchrony calculated over ±2.0 sec PEH time relative to go target presentation for trials shown in panel A.

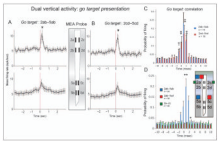

Figure 5.

Dual vertical FCx neuron firing: go target presentation. (A) Mean ± *SEM* firing rates summed over all RS FCx cells recorded in Layer 2/3 and Layer 5 during ±3.0 sec of go target presentation (0.0 sec red line) similar to Figure 3B. Firing is shown for cells recorded simultaneously at the 2ab and 5ab recording sites in the same (straight line) vertical orientation on the MEA probe. Asterisk (*) indicates significant difference between peak firing rate in Layer 2/3 sites versus lower peak rates at Layer 5 sites; Layer 2/3 peak, 10.83 ± 1.25 Hz versus Layer 5 peak, 7.09 ± 0.89, $F(1, 2486) = 4.61$, $p < .01$. (B) Mean ± *SEM* firing rates for simultaneously recorded cells in Layer 2/3 and Layer 5 recorded at the adjacent vertical oriented recording sites, 2cd and 5cd, on the MEA probe. Asterisk (*) indicates significant difference between peak mean firing rate Layer 2/3 cells versus lower peak rate for Layer 5 cells; Layer 2/3 peak, 9.01 ± 1.31 Hz versus Layer 5 peak, 6.25 ± 1.31, $F(1, 2486) = 4.44$, $p < .01$. (C) CCHs show probability of firing as mean ± *SEM* proportion of coincident Layer 5 and Layer 2/3 spikes per 1.0 msec for pairs of cells shown in panels A (blue bars) and B (red bars) recorded at each of the two parallel vertical orientations (2ab–5ab, $n = 14$ cell pairs or 2cd–5cd, $n = 18$ cell pairs) on the MEA probe. †$F(4, 1783) = 3.46$, $p < .01$; ‡$F(4, 1783) > 5.29$, $p < .001$, indicating significant increase in mean firing probability over baseline. (D) CCHs compare mean ± *SEM* firing probabilities for pairs of cells recorded from MEA sites the same ($n = 24$ pairs) vertical orientation (2ab–5ab or 2cd–5cd, blue bars, blue squares in probe diagram) or MEA sites ($n = 32$ pairs) with opposite (i.e., diagonal) vertical site orientations (2ab–5cd or 2cd–5ab, red bars, red squares in probe diagram). Asterisks (*$p < .01$, **$p < .001$) indicate significant differences in mean probability of firing for same (i.e., 2ab–5ab, blue squares) versus different (i.e., 2ab–5cd, red squares) vertically oriented cell pairs, *$F(1, 3356) > 6.7$, $p < .01$; **$F(1, 3356) > 10.8$, $p < .001$. Synchronized firing between cell pairs recorded at opposite vertical orientations (red bars) did not differ, $F(1, 1783) = 1.61$, *ns*, at any of the calculated interspike intervals (±10.0 msec). Firing of neurons recorded from the same layer but opposite vertical orientation (2a–c, green squares denote recording sites) were also not correlated, $F(1, 1783) = 1.61$, *ns* (see also Figure 2C).

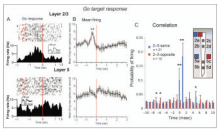

Figure 6.

Task-related FCx neuron firing: go response. (A) Single trial raster displays and PEHs for RS FCx cells recorded in Layer 2/3 (upper) and Layer 5 (lower) during the behavioral go response (red line, 0.0 sec) to go target presentation (red dots), which consisted of movement of the cursor into the go target image to a receive juice reward. Insets: waveforms (calibration = 1.0 msec, 150 μV). (B) Firing rates (mean ± *SEM*) of all FCx cells recorded in Layer 2/3 and Layer 5 summed over 2.0 sec before and 3.0 sec after completion of go target response. Asterisks indicate significant difference of mean peak increase in Layer 2/3 rate versus peak changes in Layer 5, $^{**}F(4, 2749) = 5.02$, $p < .001$. (C) CCHs comparing synchronized firing of pairs of cells in panel B recorded at either the same (2ab–5ab, 2cd–5cd; blue bars) or the opposite (diagonal: 2ab–5cd, 2cd–5ab; red bars) vertical MEA sites during go target response. Asterisks indicate significant differences in mean probability of firing, $^{*}F(1, 2117) > 7.3$, $p < .01$; $^{**}F(1, 2117) > 11.1$, $p < .001$.

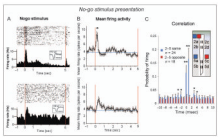

Figure 7.

Task-related FCx neuron firing: no-go stimulus presentation. (A) Firing patterns of two RS FCx pyramidal cells in Layer 2/3 (upper) and Layer 5 (lower) during no-go stimulus presentation. Single trial raster displays and PEHs (± 2.0 sec) show cell firing before and after no-go stimulus presentation (red line = 0.0 sec). Insets waveforms (calibration = 1.0 msec, 150 μV). (B) Mean ± *SEM* firing rates (±3.0 sec) for all cells recorded in Layer 2/3 (upper) and Layer 5 (lower) during no-go stimulus presentation (see Figures 3 and 5, go target presentation). Peak mean firing in Layer 2/3 cells was significantly higher than that in Layer 5 cells, $*F(1, 2883) = 7.53$, $p < .01$. No additional significant changes from baseline in mean firing rates were detected in either Layer 2/3 or Layer 5 cells during the remaining 3.5 sec of the no-go timeout interval. (C) CCHs for pairs of cells recorded in panel B during no-go stimulus presentation at MEA sites with the same (2ab–5ab, 2cd–5cd) or opposite (2ab–5cd, 2cd–5ab) vertical orientations. Asterisks indicate comparison of same versus opposite vertical orientation sites, $*F(1, 2306) > 6.8$, $p < .01$; $**F(1, 2306) > 10.9$, $p < .001$.

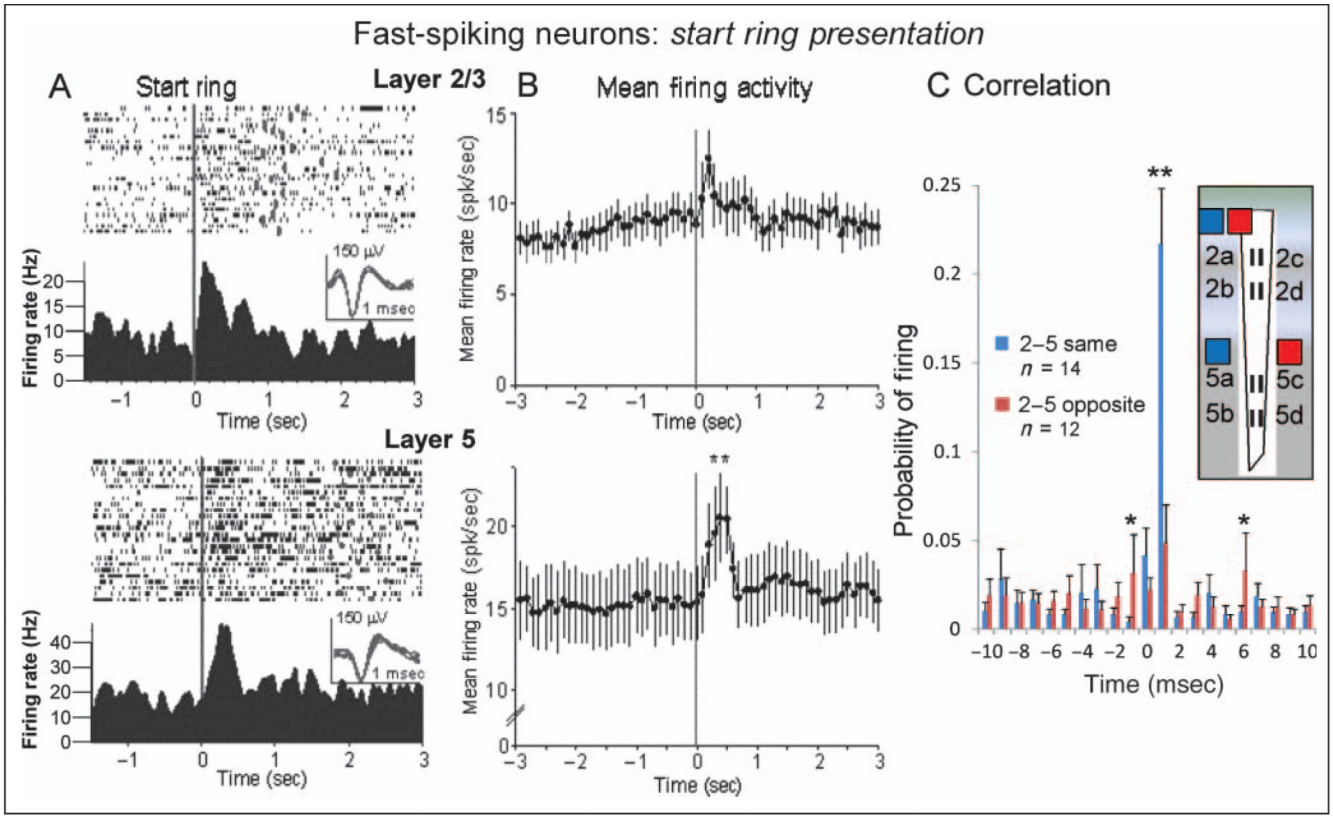

Figure 8.

FS Neurons in FCx: start ring presentation. (A) Single trial raster displays and PEHs show firing patterns of two FS FCx neurons recorded from Layer 2/3 (upper) and Layer 5 (lower), respectively, during start ring presentation (see Figure 3). Insets: waveforms for each FS cell (calibration = 1.0 msec, 150 µV). (B) Mean ± *SEM* firing rates summed over all FS cells recorded in Layer 2/3 (upper) and Layer 5 (lower) during presentation of start ring image (black line at 0.0 sec). Layer 5 FS cells showed a greater mean peak increase at 0.5 sec after the start ring presentation (21.47 ± 2.83 Hz) relative to prepresentation baseline (−2.0 sec) rate (14.62 ± 0.29 Hz) than Layer 2/3 FS cells (12.47 ± 2.11 Hz) relative to their respective baseline (8.13 ± 0.37 Hz) firing rate, **$F(1, 3388) = 10.13$, $p < .001$. (C) CCHs for pairs of fast-spiking cells recorded in panel B during start ring presentation at sites on the recording MEA with the same (2ab–5ab, 2cd–5cd) or opposite (2ab–5cd, 2cd–5ab) vertical orientations. Asterisks indicate minimal mean values for significance levels of *$F(1, 1916) > 7.1$, $p < .01$, **$F(1, 1916) > 11.3$, $p < .001$.

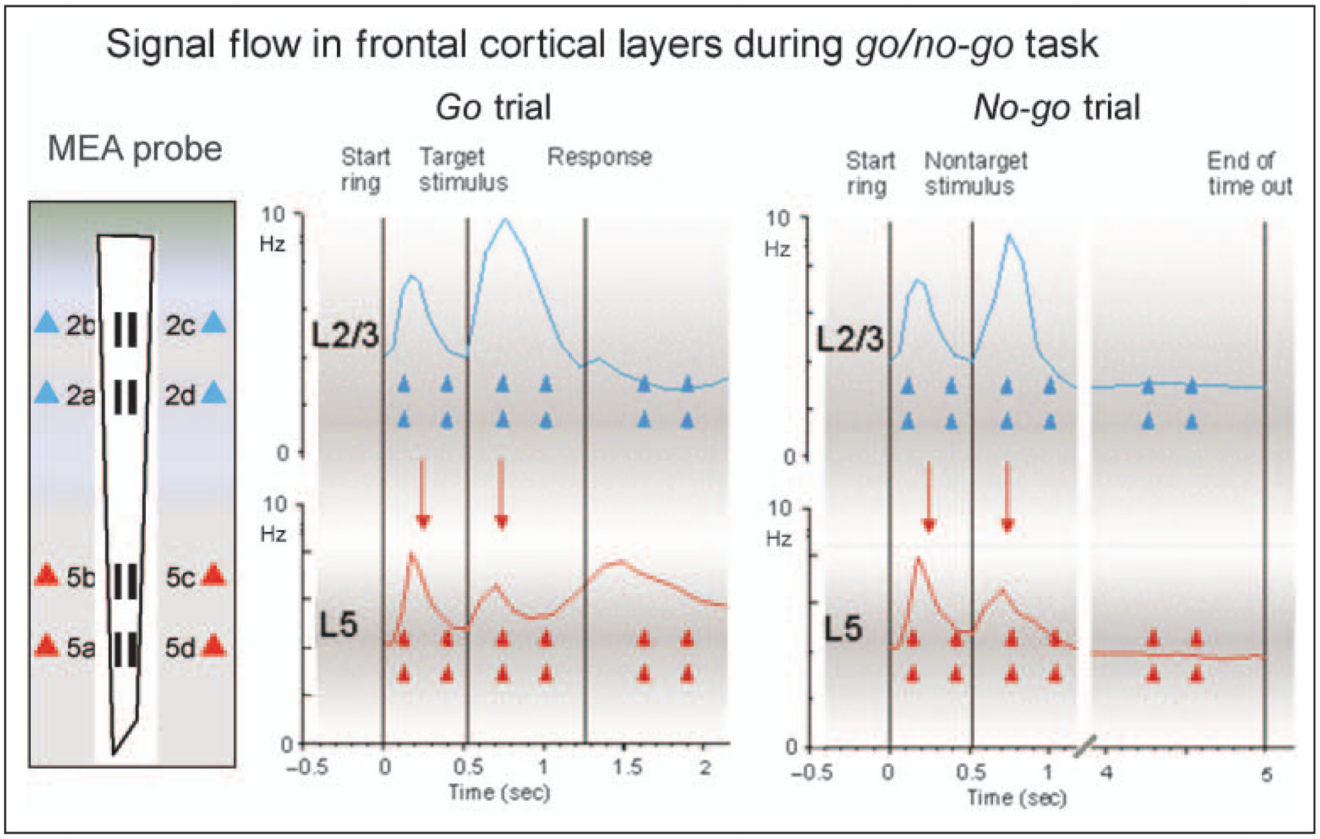

Figure 9.

Task-related signal processing in frontal cortical cell layers. MEA probe: Diagram of conformal MEA at left shows recording arrangement that allowed determination of correspondence between task-related firing in Layer 2/3 cells (blue triangles) and Layer 5 cells (red triangles) in NHPs during performance of go/no-go task. Go trial: Composite mean firing profile of cells over the time course of a go target trial in which Layer 2/3 cells (blue trace) and Layer 5 cells (red trace) were sequentially activated by task-relevant stimuli (start ring, go target presentation, and response). No-go trial: Diagram depicts the same events for a *no-go* trial showing composite mean firing of Layer 2/3 (blue trace) and Layer 5 (red trace) cells was similar to *go* Trials but with no differential firing between layers during the *no-go timeout* interval. The demonstrated synergy of the excitatory peaks between cells in Layer 2/3 and Layer 5 during task-related events (downward red arrows) is consistent with proposed top–down flow of sensorimotor information (Weiler et al., 2008; Yoshimura et al., 2005; Lebedev et al., 2002), indicative of “columnar readout” of the two distinct motor plans required on *go* and *no-go* trials.

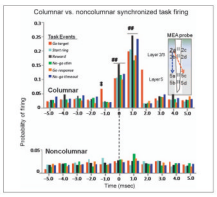

Figure 10.

Specificity of columnar processing of task-related information in FCx layers. Composite CCHs for all FCx cells recorded in each task-related event partitioned with respect to Layer 2/3 and Layer 5 cell pairs recorded from either the same or the opposite vertically oriented recording sites on the conformal MEA illustrated in diagram at right. Columnar (upper) CCHs show synergistic firing (increased mean firing probabilities) between pairs of cells recorded at sites with the same (2ab–5ab, 2cd–5cd) vertical orientation on the MEA. Task events are listed for each color of bar. Noncolumnar CCHs (lower) show that under no task-related conditions (events) did Layer 5 cells recorded at opposite (i.e., diagonal) vertical orientations on the MEA (2ab–5cd or 2cd–5ab) fire in a synergistic manner with Layer 2/3 cells. The CCHs provide strong evidence for “minicolumnar” processing of task-relevant information (Weiler et al., 2008). Symbols (##) indicate comparison of columnar (blue dotted arrow) versus noncolumnar (red dotted arrow) synchrony at ±1.0 msec, $F(1, 2117) > 11.1$, $p < .001$. Symbol (‡) indicates minimal increase in synchrony (mean ± *SEM* firing probability) above background level (±6.0 msec) required to achieve significance, $F(4, 1783) > 5.03$, $p < .001$. CCH data for go target presentation, go target response, and no-go stimulus as shown in Figures 3–8, with time scale shortened to ±5.0 msec.